



Conference Proceedings of the 5th Asia Pacific Luminescence and Electron Spin Resonance Dating Conference
October 15th-17th, 2018, Beijing, China

Guest Editor: Barbara Mauz

COMPONENT RESOLVED EQUIVALENT DOSE ESTIMATION USING TL GLOW CURVES OF TRAVERTINE SAMPLES FROM ANATOLIA, TURKEY

EREN ŞAHINER^{1,2}, GEORGE S. POLYMERIS^{1,2}, M. ZEYNEL ÖZTÜRK³,
Y. KAĞAN KADIOĞLU² and NIYAZI MERİÇ^{1,2}

¹Institute of Nuclear Sciences, Ankara University, Beşevler 06100, Ankara, Turkey

²Earth Sciences Application and Research Center of Ankara University (YEBİM), Gölbaşı 06830, Ankara, Turkey

³Niğde Ömer Halisdemir University, Department of Geography, 51240, Niğde, Turkey

Received 19 January 2019

Accepted 12 July 2019

Abstract This study provides methodological aspects on the equivalent dose estimation for travertine samples, namely heated calcium carbonate, using the TL multiple-aliquot additive-dose approach. Large equivalent doses (EDs), within the range 750–1300 Gy, were calculated using the plateau method based on the NTL glow curve. Moreover, a component resolved TL glow-peak analysis was carried out, using the integrated intensity of the NTL glow peaks for the ED estimation after deconvolution based on the OTOR model. Three different TL peaks were used, termed P4, P5 and P6. The integrated intensity of TL glow peak P4 resulted in age overestimation (15–26%), compared to the age provided using the plateau method. This overestimation could be attributed to the fact that the temperature range of P4 does not coincide with the plateau region of each sample. Milder overestimation (8–14%) was noticed using the integrated intensity of TL glow peak P6, mostly due to the poor deconvolution resolution. Only the integrated intensity of TL glow peak P5 after deconvolution provides ED values compatible with those yielded using the plateau method, with good accuracy. The present study suggests not using the TL intensity (neither in terms of integrated intensity nor of peak height intensity) for ED estimation; instead it is highly recommended to use either the plateau method, or alternatively integrated intensity of TL peak P5 after deconvolution. Unfortunately, using the peak height of TL P5 is not recommended, due to overlapping with P6.

Keywords: Equivalent dose, thermoluminescence dating, travertine, deconvolution, Calcium carbonate, luminescence dating.

1. INTRODUCTION

Calcium carbonate, with the chemical formula CaCO_3 , stands among the most widespread minerals of earth's crust. The importance of dating calcium carbonate based formations for setting age limits has been well demonstrated by both the uranium series disequilibrium method as well as Electron Paramagnetic Resonance (EPR) techniques. As far as luminescence techniques are concerned, Wintle (1977, 1978) has undertaken some of the initial work to assess whether the TL signal from calcite could be used to date geologically relevant samples. The reader may also refer to McDougal (1968) for a review of earlier achievements on this related topic. Due to the problematic properties, or even the lack, of optically stimulated luminescence (OSL) signal, thermoluminescence (TL) stands as the only luminescence technique available for dating applications for these formations.

Despite the numerous reports dealing with the EPR dating applications of calcium carbonates (for example Ikeya, 1993 and references therein), a limited number of papers deal with the corresponding luminescence applications of this mineral within the last 35 years (Debenham, 1983; Debenham and Aitken, 1984; Down *et al.*, 1985; Ninagawa, 1987; Ninagawa *et al.*, 1988, 1992; Liritzis, 1989; 2010; 2011; Duller *et al.*, 2009; Stirling *et al.*, 2014; Polymeris *et al.*, 2016), both successful and unsuccessful. Throughout this aforementioned literature, the TL properties of various types of CaCO_3 samples have been reported and the ages were in most cases lower than 500 ka. The present study provides methodological aspects on the ED estimation using the multiple-aliquot additive-dose procedure in the TL of calcium carbonate samples. Two different alternative approaches were adopted, namely a TL peak resolved analysis following deconvolution and the plateau method without deconvolution. Four different samples from the Quaternary were studied.

2. MATERIALS AND METHODS

Apparatus

All luminescence measurements were conducted using a commercial Risø TL/OSL system (model TL/OSL-DA-20), equipped with blue LEDs (470 nm, FWHM 20 nm) and a $^{90}\text{Sr}/^{90}\text{Y}$ beta particle source, delivering a nominal dose rate of 0.1083 Gy/s. An EMI 9235QB photomultiplier tube was used for the detection of all luminescence signals. For the cases of the few OSL and TA – OSL measurements, a Hoya (U-340) filter was used for light detection (340 nm, FWHM 80nm) while for all TL measurements only a BG-39 glass filter was used to restrict the wavelengths detected, similar to the studies of Duller *et al.*, (2009) as well as of Polymeris *et al.* (2016). This filter has a transmission window that ranges from 350 to 600 nm and it was used for all TL measurements. All heatings and TL measurements were performed in a

nitrogen atmosphere using a low constant heating rate of 2°C/s in order to avoid significant temperature lag (Kitis *et al.*, 2015); the samples were heated up to the maximum temperature of 500°C . All luminescence measurements were conducted at the Institute of Nuclear Sciences of Ankara University.

For the structural characterization of the materials, the X-ray powder diffraction (XRPD) technique was applied; the minerals were analyzed to verify their crystalline structure using a Philips diffractometer with monochromatic $\text{CuK}\alpha$ ($\lambda = 0.15406$ nm) radiation. For a description of the elemental-chemical composition of the samples, Polarized Energy Dispersive X-ray fluorescence (XRF) analysis was performed using an X-ray Fluorescence spectrometer Spectro XLAB-2000. Both PXRD and XRF measurements and analysis were performed at the Earth Sciences Application and Research Center of Ankara University (YEBIM).

Materials and treatment

In this work, four different travertine samples were collected from the Bor district of Niğde city, Central Anatolia, Turkey. Travertine deposits are the product of calcium carbonate precipitation under cool water (Ford and Pedley, 1996). The thickness of the deposits differs between 15 and 25 meters. These deposits are considered belonging to the Quaternary, based on indirect proxies as well as preliminary luminescence dating results (Öztürk *et al.*, 2018). The Southern part of study area was bordered with Bor Segment of Tuzgözü (Saltlake) Fault Zone, Turkey.

Based on Electron dispersion X-ray (EDX) spectroscopy, all samples contain predominantly Ca (38.85%), O (37.87%), while to a lesser extent C (21.03%); all percentage values indicate average values over all samples of the present study. This observation is in excellent agreement with the results of X-ray powder diffraction (XRPD) patterns, indicating the presence of the phase of CaCO_3 solely. The sample codes as well as the concentration of each main element are presented in **Table 1** for each sample. Typically, travertines are formed where cool carbonate supersaturated freshwater degasses and this is where karst water reaches the surface. Thus, various impurities are expected into the otherwise clean CaCO_3 precipitate. **Table 1** also presents the XRF results for other available elements as well, including K, Na, Fe, Mg, Mn, Si, Al, Ti and Cl. In some cases, the corresponding concentrations are below the detection limit of the PXRD technique.

Before luminescence measurements, treatments and preparation were under-taken in subdued red filtered light conditions. An almost 1 cm thick, outer layer was removed from each sample in the laboratory, to eliminate the light-subjected parts of the samples. Finally, grains with dimensions in the range 4–12 μm were extracted by gently crushing in an agate pestle and mortar, then suspended in acetone and finally precipitated onto 1 cm

Table 1. Content of main elements. The detection limit for the (%) concentration is 0.01%. BDL=Below Detection Limits.

A/A	Sample Codes	Ca content (%)	C content (%)	O ₂ content (%)	K content (%)	Na content (%)	Fe content (%)	Mg content (%)	Mn content (%)	Si content (%)	Al content (%)	Ti content (%)	Cl content (%)
1	SB1	40.15	37.44	20.53	BDL	0.05	0.51	0.26	0.03	0.13	0.76	0.09	BDL
2	SB2	37.41	38.84	21.23	BDL	0.07	0.41	0.18	BDL	0.32	0.71	0.71	0.06
3	SB3	39.05	38.15	20.28	BDL	BDL	0.61	0.77	0.07	0.21	0.33	0.51	0.03
4	SB4	38.79	37.05	22.07	BDL	0.03	0.53	0.58	0.08	0.14	0.19	0.48	0.05

diameter aluminum discs (Fleming, 1979). As PXRD indicated the presence of solely CaCO₃, no further chemical procedure was applied.

Methods of analysis

For the equivalent dose estimation the multiple aliquot additive dose procedure (MAAD) in TL was applied. A detailed description of the procedure can be found in Aitken (1985; 1998), Wagner (1998) and Liritzis *et al.* (2013). Mass reproducibility for all discs-aliquots was kept within ±3%. The additive doses applied were 0 (NTL), 150, 300, 450, 600 and 900 Gy. Four fresh aliquots were used for each additive dose. The equivalent dose (ED) was calculated using two different approaches. For the first approach, the ED was calculated using the plateau method (Aitken, 1985; Wagner, 1998) according to the following equation (Liritzis, 2010; Liritzis *et al.*, 2015; Aidona *et al.*, 2018):

$$ED = \frac{NTL}{(NTL + \beta_i) - NTL} \cdot \beta_i = \frac{NTL}{S_i} \quad (2.1)$$

where NTL is the natural TL glow curves, (NTL + β_i) denotes the glow curves after the beta doses were added on top of the natural signal and β_i the corresponding administered beta dose in units of Gy. S_i denotes the slope of the (linear) fitting of the dose response curve and is defined according to the following equation (Polymeris *et al.*, 2012; Liritzis *et al.*, 2015):

$$S_i = \frac{(NTL + \beta_i) - NTL}{\beta_i} \quad (2.2)$$

Eqs. 2.1 and 2.2 were applied to the entire NTL and NTL + β_i glow curves. Since all TL curves were measured using 500 data points and heating rate of 1°C/s up to a maximum temperature of 500°C, the preceding calculations take place for each data point of the glow curves. Eventually Eq. 2.2 gives five different curves, each one corresponding to one among the additive doses applied with each data point corresponding to a different temperature in steps of 1°C. In the case of linearity, these five curves should coincide, at least in a selected glow curve temperature range. For this temperature range, the ED is independent on the selection of the integration limits of the TL signal; therefore, if one plots the ED versus the TL glow curve temperature range, a plateau region is yielded. So the ED is calculated within this temperature range, which is specified experimentally.

However, this latter approach does not provide TL peak resolved analysis, but just a plateau within a temperature range within the glow curve. In order to get TL peak-resolved analysis, a computerized glow curve deconvolution analysis was applied to all experimental TL glow curves, using the OTOR model (Halperin and Braner, 1960) and the analytical solution of the corresponding differential equations. ED was calculated using the integral of each TL peak after deconvolution analysis. The equations applied for the deconvolution analysis were the following (Sadek *et al.*, 2014):

$$I(T) = I_m \exp\left(-\frac{E}{kT} \cdot \frac{T_m - T}{T_m}\right) \cdot \frac{W(z_m) + W(z_m)^2}{W(z) + W(z)^2} \quad (2.3)$$

where $W(z)$ is the Lambert function; z , being the independent variable of the equations, is approximated by the expression:

$$z = \exp\left(\frac{R}{1-R} - \ln\left(\frac{1-R}{R}\right) + \frac{E \cdot \exp\left(\frac{E}{kT_m}\right)}{kT_m^2(1-1.05 \cdot R^{1.26})} \cdot F(T, E)\right) \quad (2.4)$$

and z_m is the value of z from the above equation, for $T = T_m$.

These Eqs. 2.2 and 2.3 are the analytical equations used to fit the experimental TL glow curves, with the two adjustable fitting parameters being the activation energy E and the ratio R (with $R < 1$) (Kitis and Vlachos, 2012). The value of the parameter R indicates the order of kinetics; R value close to 0 indicates first order of kinetics, while a value close to 1 indicates second order of kinetics (Şahiner, 2017). The function $F(T, E)$ in this expression is the exponential integral appearing in TL models and is expressed in terms of the exponential integral function $Ei[-E/kT]$ as (Chen and McKeever, 1997; Kitis *et al.*, 2006):

$$F(T, E) = \int_{T_0}^T e^{-\frac{E}{kT}} dT = T \cdot \exp\left(-\frac{E}{kT}\right) + \frac{E}{k} \cdot Ei\left[-\frac{E}{kT}\right] \quad (2.5)$$

The software package Microsoft Excel was used for the deconvolution analysis, using the Solver utility (Afouxenidis *et al.*, 2012), while the goodness of fit was tested using the Figure Of Merit (FOM) of Balian and Eddy (1977) given by:

$$FOM(\%) = 100 * \sum_p |TL_{\text{exp}} - TL_{\text{fit}}| / \sum_p TL_{\text{fit}} \quad (2.6)$$

The FOM index value provides a measure for the goodness of fit; the lowest its value, the best fit it is. Therefore, every fitting attempt results in minimizing the FOM index value, which was achieved by changing the

set of the parameter values of each glow peak. FOM values in all cases were less than 0.9%, indicating the fitting quality.

3. RESULTS AND DISCUSSION

OSL and TA-OSL signals

Fig. 1 presents typical OSL as well as thermally assisted optically stimulated luminescence (TA – OSL, Polymeris, 2016) signals from one CaCO_3 sample of the present study following natural irradiation, namely without any artificial irradiation in the laboratory. The OSL signal was measured at 110°C , while the TA – OSL at 200°C . It is obvious from this figure that both signals consist of one component with shape rather peculiar and extremely flat. In terms of intensity levels, while the OSL indicates a signal similar to background, the TA – OSL yields intensity as large as ~ 18 times the OSL background signal. As this figure reveals, a fast decaying component is missing from both signals. Neither the intensity nor the shapes of both OSL signals do change, even after illumination up to 1 ks using blue LEDs. This result indicates that these signals are extremely hard to bleach, at least within relative short time intervals. These features stand as indirect indications regarding the lack of significant quantities of either quartz or feldspar inclusions inside the clear CaCO_3 precipitate. The lack of both quartz and feldspar inclusions could be further supported by the contents of Si and Na/K respectively, according to **Table 1**. In agreement with the previous reports by both Liritzis (1989; 2000; 2011) and Galloway (2002) we conclude that both OSL signals are not useful for luminescence dating. This is the reason why, for dating applications, the luminescence applications to calcium car-

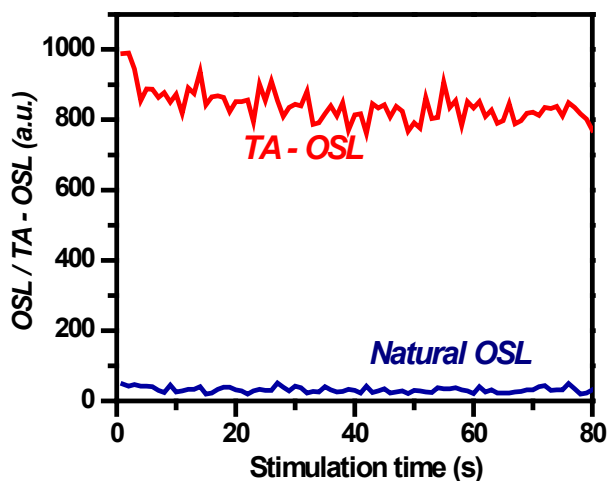


Fig. 1. Representative natural OSL and thermally assisted OSL (TA – OSL) signals corresponding to the CaCO_3 sample with code SB3. These signals are not useful for dating applications.

bonates so far were limited to TL of mostly biogenic calcite (Duller *et al.*, 2009; Liritzis, 2010; 2011; Polymeris *et al.*, 2016). The TL signal of CaCO_3 samples is known to be bleachable, however, prolonged bleaching times are required (hours or even days, McDougal, 1968; Liritzis, 1989; 2000). For a recent, indicative example, the authors could refer to **Fig. 6** of Polymeris *et al.* (2016).

ED determination using the plateau method

The natural TL glow curves of all samples exhibit the same main characteristics, namely a glow curve that has the form of a continuum with two distinct but overlapping TL peaks at 325°C and at 450°C (**Fig. 2a**). **Figs. 2b** and **2c** present the MAAD TL analysis results for the sample SB1, which are representative for all the samples that were subject to the present study.

Fig. 2b presents the curves corresponding to the dose–response slopes (S_i) which are plotted versus temperature for a selection of different additive doses applied for the sample SB1. S_i curves were calculated according to **Eq. 2.2** and the preceding subtraction takes place for each data point of the glow curves. According to **Fig. 2b**, these S_i curves coincide, throughout a wide temperature region of the glow curve, namely between 250°C and 400°C , confirming thus the dose response linearity within this aforementioned temperature range, despite the large additive doses. Consequently, the ED plateau is expected within the temperature range between 250°C and 400°C . Similar linearity S_i features were also indicated for the rest of the samples.

Equivalent doses were calculated using **Eq. 2.1**. Since (a) all TL curves were measured using 500 data points and heating rate of 1°C/s up to a maximum temperature of 500°C and (b) the calculations take place for each data point of the glow curves, an ED value correspond to each TL glow curve temperature. If one plots these ED values versus the TL temperature, an ED plateau is expected to occur. A typical plot of ED plateau against glow curve temperature is presented in **Fig. 2c**. Errors, which are derived mainly from the uncertainties in curve fitting, are $\pm 1\sigma$ and were calculated by standard error propagation analysis. In all cases, ED plateaus are wide enough, over 100°C wide. The equivalent doses were obtained as the mean values of the plateaus for each sample. Quite large ED values were obtained, ranging between $781(\pm 71)$ and $1458(\pm 166)$ Gy. Only linear fittings were performed to the dose response curves. Details of this ED calculation, such as the length, the value and the error of each ED plateau are presented for all samples in **Table 2**. It is worth emphasizing that for the estimation of the ED plateau region, all reheats (background TL glow curves) were subtracted. Moreover, for all samples the temperature range corresponding to the ED plateau lies within the temperature range of linearity according to the S_i curves. Low dose supralinearity was not observed.

Deconvolution results and component resolved ED estimation

Fig. 3 presents a NTL + β (450 Gy) glow curve, deconvolved into its individual TL peaks according to **Eqs. 2.3–2.5**. For all NTL + β_i glow curves, six individual TL glow peaks were used in order to achieve fit of excellent

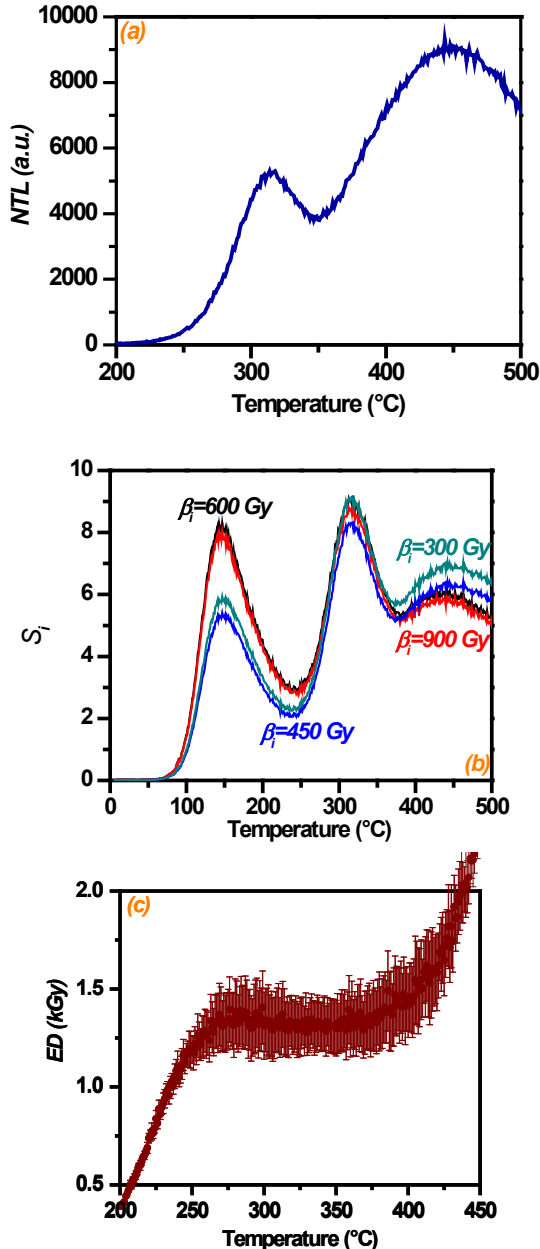


Fig. 2. Typical results of the MAAD plateau method applied for sample SB1. Plot (a) presents a NTL glow curve (as an average of three independently measured glow curves), plot (b) presents the representative S_i curves for a selection of additive doses according to equation (2) while plot (c) presents an ED plateau versus glow curve temperature according to equation (1). Error bars correspond to 1σ .

quality (FOM <0.9%). Nevertheless, for the case of the NTL glow curves, only three TL glow peaks are required (namely P4, P5 and P6) in order to achieve fit of excellent quality. A TL background curve has also been included within the deconvolution procedure, as **Fig. 3** indicates. **Table 3** presents an outline of the deconvolution analysis results, including the values of T_{max} , activation energy E and the parameter R which gives information on the order of kinetics. It should be emphasized that the results obtained for all four samples studied were similar. The reproducibility of the T_{max} values with ranging additive doses stands in excellent agreement with the R values of <0.1. Moreover, based on the deconvolution results, the lifetimes of the TL traps included in the NTL glow curves are adequate enough for providing ages of the order of 1 Ma.

Besides the ED plateau method, equivalent doses were also calculated using the integrated TL intensity of each one of the three TL glow peaks which were used to deconvolve the NTL glow curves. An outline of the TL peak resolved ED estimation results could be found in **Table 2**. TL glow peak P4 is quite prominent, indicating very intense signal. The fitting parameters corresponding to this specific TL peak yield the lowest error values. However, the equivalent dose values calculated using the deconvolved integrated specific TL peak are overestimated when compared to the ED plateau value. **Fig. 4** presents a representative additive dose response curve corresponding to sample SB1, plotted for the case of the integrated intensity of TL glow peak P4 after deconvolution.

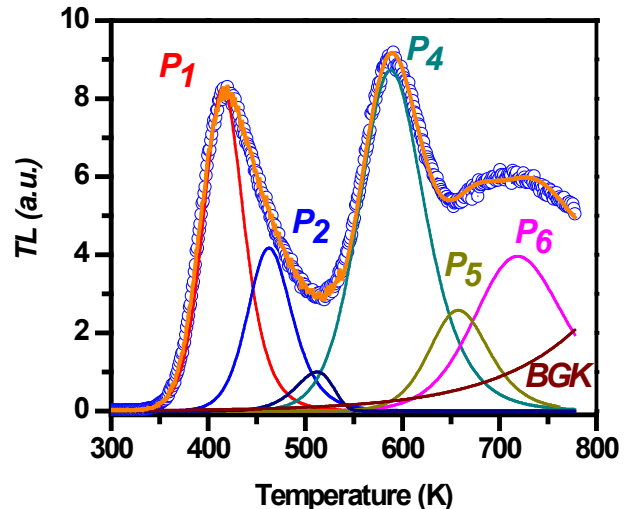


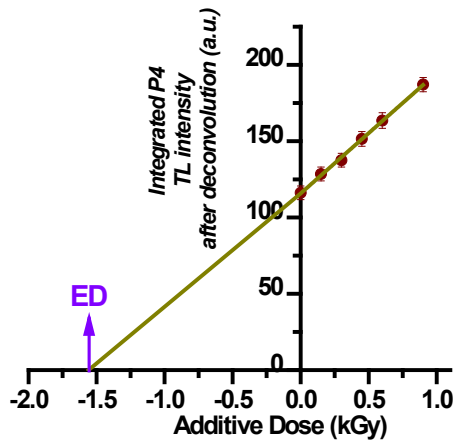
Fig. 3. Representative deconvolution analysis of a TL glow curve corresponding to the sample SB1, after a dose of 450 Gy (open data points). Six different TL glow peaks and a black body radiation curve (BGK) were used in order to fit the experimental glow curve. Each TL glow peak is presented in solid line and is denoted as P_i . Orange solid line indicates the fitting curve. **Table 2** indicates the activation energies of the TL peaks.

Table 2. Data related to the ED estimation for all four samples.

A/A	Sample Codes	Plateau ΔT (°C)	Plateau ED (Gy)	P4 ED (Gy)	P5 ED (Gy)	P6 ED (Gy)
1	SB1	270–370	1258 ± 155	1578 ± 171	1312 ± 137	1422 ± 158
2	SB2	280–385	1458 ± 166	1682 ± 149	1489 ± 155	1358 ± 185
3	SB3	260–380	1077 ± 91	1236 ± 133	1113 ± 107	1193 ± 128
4	SB4	270–380	781 ± 70	932 ± 98	812 ± 86	850 ± 88

Table 3. Deconvolution results for fitting parameters of all four samples.

A/A	Sample Codes	P4 T_{max} (°C)	P4 R	P4 E (eV)	P5 T_{max} (°C)	P5 R	P5 E (eV)	P6 T_{max} (°C)	P6 R	P6 E (eV)
1	SB1	328 ± 4	0.06	1.34 ± 0.12	399 ± 11	0.09	1.59 ± 0.18	453 ± 22	0.01	1.81 ± 0.21
2	SB2	326 ± 5	0.04	1.37 ± 0.11	402 ± 10	0.05	1.63 ± 0.17	457 ± 21	0.01	1.86 ± 0.19
3	SB3	328 ± 3	0.09	1.34 ± 0.13	404 ± 13	0.07	1.64 ± 0.16	463 ± 22	0.02	1.88 ± 0.24
4	SB4	327 ± 5	0.05	1.41 ± 0.12	402 ± 13	0.05	1.61 ± 0.17	459 ± 24	0.01	1.79 ± 0.20


Fig. 4. Representative additive dose growth curve in terms of the integrated intensity of TL glow peak P4 after deconvolution, for the sample with code SB1. The arrow indicates the ED value.

Despite the fact that the additive doses extend up to 900 Gy, linearity of the TL signal is characteristic for all samples. ED is overestimated at 1578(±177) Gy, while the corresponding plateau ED was calculated as 1258(±155) Gy. Similar overestimation was also yielded while using solely the integral of P6 TL peak. Component resolved overestimation ranges between 8 and 26%, depending on the TL peak used. Nevertheless, the most prominent TL glow peak P4 yields the higher overestimation percentage (15–26%). This experimental overestimation could be attributed to the fact that temperature range of TL glow peak P4 does not coincide with the plateau region for all samples. The overestimation yielded using TL glow peak P6, ranging between 8–14%, could be attributed to the fact that the TL glow curve should be measured up to temperatures higher than 500°C. As this

is not the case, the resolution of the deconvolution technique is not the optimum. On the contrary, the additive dose procedure using the TL glow peak P5 yields the most comparable ED results with the ED plateau methodology. This similarity is quite prominent from the results of **Table 1** and it is attributed to the fact that TL peak P5 lies within the corresponding plateau temperature range. Once again, it is worth noting that for all four samples and all three TL peaks, the linearity is quite impressive, despite the high additive doses applied.

TL ages

Estimation of the uranium, thorium and potassium geochemical content of the samples in the present study is currently pending. According to previous related luminescence studies using CaCO₃, this geochemical content is quite low, indicating annual dose rate values lower than 1Gy/ka (for example Liritzis, 2010; 2011; Polymeris *et al.*, 2016). Based on this rationale, the TL ages of these samples could reach values at least of 1 Ma, or even higher, namely in the Quaternary era. Nevertheless, as the present manuscript aims at presenting methodological aspects, as it was the case of the report by Duller *et al.*, (2009), the detailed presentation of an integrated study dealing with the ages and their geological implications will be presented elsewhere.

4. CONCLUSIONS

- The present study provides methodological aspects on the ED estimation for travertine samples, namely calcium carbonate samples, using the multiple-aliquot additive-dose procedure in TL.
- Heated CaCO₃ can be effectively used for calculating equivalent doses within the range 750–1300 Gy.
- OSL and TA – OSL curves were measured and proven inappropriate for age assessment.

- The integrated intensity of TL glow peak P4 after deconvolution, provides age overestimation, compared to the age provided using the plateau method. This overestimation could be attributed to the fact that temperature range of P4 does not coincide with the plateau region of each sample.
- Using the integrated intensity of TL glow peak P6 after deconvolution is not suggested, as the resolution for resolving this peak is not good. As a result of this poor resolution, ED overestimation is also monitored.
- The integrated intensity of TL glow peak P5 after deconvolution provides ED values compatible with those yielded using the plateau methodology within the entire TL glow curve, with better accuracy, namely lower error values.
- The present study suggests not using the TL intensity (neither in terms of integrated intensity nor of peak height intensity) for ED estimation; instead it is highly recommended to use either the plateau methodology, or alternatively integrated intensity of TL peak P5 after deconvolution. Unfortunately, using the peak height of TL P5 is not recommended, due to overlapping with P6.
- TL age results indicate a formation during the Quaternary.

REFERENCES

- Afouxenidis D, Polymeris GS, Tsirliganis NC and Kitis G, 2012. Computerised curve deconvolution of TL/OSL curves using a popular spreadsheet program. *Radiation Protection Dosimetry* 149(3): 363–370, DOI 10.1093/rpd/ncr315.
- Aidona E, Polymeris GS, Camps P, Kondopoulou D, Ioannidis N and Raptis K, 2018. Archaeomagnetic versus luminescence methods: the case of an Early Byzantine ceramic workshop in Thessaloniki, Greece. *Archaeological and Anthropological Sciences* 10: 725–741, DOI 10.1007/s12520-017-0494-5.
- Aitken MJ, 1985. *Thermoluminescence dating*. Academic Press, London.
- Aitken MJ, 1998. *An introduction to optical dating: the dating of quaternary sediments by the use of photon-stimulated luminescence*. Oxford University Press.
- Balian HG and Eddy NW, 1977. Figure Of Merit (FOM): an improved criterion over the normalized chi-square test for assign the goodness-of-fit of gamma ray spectral peaks. *Nuclear Instruments and Methods* 145, 389–395, DOI 10.1016/0029-554X(77)90437-2.
- Chen R and McKeever SWS, 1997. *Theory of Thermoluminescence and Related Phenomena*. World Scientific.
- Debenham NC, 1983. Reliability of thermoluminescence dating of stalagmitic calcite. *Nature* 304: 154–156, DOI 10.1038/304154a0.
- Debenham NC and Aitken MJ, 1984. Thermoluminescence dating of stalagmitic calcite. *Archaeometry* 26: 155–170, DOI 10.1111/j.1475-4754.1984.tb00330.x.
- Down JS, Flower R, Strain JA and Townsend PD, 1985. Thermoluminescence emission spectra of calcite and Iceland spar. *Nuclear Tracks and Radiation Measurements* 10: 581–589, DOI 10.1016/0735-245X(85)90061-4.
- Duller GAT, Penkman KEH and Wintle AG, 2009. Assessing the potential for using biogenic calcites as dosimeters for luminescence dating. *Radiation Measurements* 44: 429–433, DOI 10.1016/j.radmeas.2009.02.008.
- Fleming S, 1979. *Thermoluminescence techniques in archaeology*. Clarendon Press.
- Ford TD and Pedley HM, 1996. A review of tufa and travertine deposits of the world. *Earth-Science Reviews* 41(3–4): 117–175, DOI 10.1016/S0012-8252(96)00030-X.
- Galloway RB, 2002. Does limestone show useful optically stimulated luminescence? *Ancient TL* 20: 1–7.
- Halperin A and Braner AA, 1960. Evaluation of thermal activation energies from glow curves. *Physical Review* 117: 408–415, DOI 10.1103/PhysRev.117.408.
- Ikeya M, 1993. *New Applications of Electron Spin Resonance: Dating, Dosimetry and Microscopy*. World Scientific, Singapore.
- Kitis G, Chen R, Pagonis V, Carinou E and Kamenopoulou V, 2006. Thermoluminescence under an exponential heating function: I. Theory. *Journal Of Physics D: Applied Physics* 39: 1500–1507, DOI 10.1088/0022-3727/39/8/008.
- Kitis G and Vlachos ND, 2012. General semi-analytical expressions for TL, OSL and other luminescence stimulation modes derived from the OTOR model using the Lambert W-function. *Radiation Measurements* 48: 47–54, DOI 10.1016/j.radmeas.2012.09.006.
- Kitis G, Kiyak NG and Polymeris GS, 2015. Temperature lags of luminescence measurements in a commercial luminescence reader. *Nuclear Instruments and Methods in Physics Research Section B: Beam Interactions with Materials and Atoms* 359: 60–63, DOI 10.1016/j.nimb.2015.07.041.
- Liritzis I, 2000. Advances in thermo- and opto- luminescence dating of environmental materials (sedimentary deposits): part II: applications. *Global Nest* 2(1): 29–49.
- Liritzis I, 2010. Strofilas (Andros Island, Greece): new evidence for the cycladic final neolithic period through novel dating methods using luminescence and obsidian hydration. *Journal of Archaeological Science* 37: 1367–1377, DOI 10.1016/j.jas.2009.12.041.
- Liritzis I, 2011. Surface dating by luminescence: an overview. *Geochronometria* 38: 292–302, DOI 10.2478/s13386-011-0032-7.
- Liritzis Y, 1989. Dating of calcites: some aspects of radiation survey in caves and dose-rates. *Bulletin Geologique des Pays Helleniques* 34(1): 123–136.
- Liritzis I, Singhvi AK, Feathers JK, Wagner GA, Kadereit A, Zacharias N and Li SH, 2013. *Luminescence Dating in Archaeology, Anthropology and Geoarchaeology: an Overview*. Springer Briefs in Earth System Sciences. Springer, Heidelberg. DOI 10.1007/978-3-319-00170-8.
- Liritzis I, Aravantinos V, Polymeris GS, Zacharias N, Fappas I, Agiamarniotis G, Sfampa IK, Vafiadou A and Kitis G, 2015. Witnessing prehistoric Delphi by luminescence dating. *Comptes Rendus Palevol* 14: 219–232, DOI 10.1016/j.crpv.2014.12.007.
- McDougal DJ, 1968. *Thermoluminescence of Geological Materials*. London University Press.
- Ninagawa K, 1987. Thermoluminescence dating of fossil calcite shells. *Japanese Journal of Applied Physics* 26: 2127–2133, DOI 10.1143/JJAP.26.2127.
- Ninagawa K, Adachi K, Uchimura N, Yamamoto I, Wada T, Yamashita Y, Takashima I, Sekimoto K and Hasegawa H, 1992. Thermoluminescence dating of calcite shells in the Pectinidae family. *Quaternary Science Reviews* 11: 121–126, DOI 10.1016/0277-3791(92)90052-A.
- Ninagawa K, Takahashi N, Wada T, Yamamoto I, Yamashita N and Yamashita Y, 1988. Thermoluminescence measurements of a calcite shell for dating. *Quaternary Science Reviews* 7: 367–371, DOI 10.1016/0277-3791(88)90031-5.
- Öztürk MZ, Şener MF and Şahiner E, 2018. Quaternary slip-rates of the Bor segment of Tuzgölü fault zone. *Omer Halisdemir University Journal of Engineering Sciences* 7(3): 1049–1053 (In Turkish).
- Polymeris GS, 2016. Thermally assisted OSL (TA-OSL) from various luminescence phosphors; an overview. *Radiation Measurements* 90: 145–152, DOI 10.1016/j.radmeas.2016.01.035.
- Polymeris GS, Erginal AE and Kiyak NG, 2012. A comparative morphological, compositional and TL study of Tenedos (Bozcaada) and Şile aeolianites, Turkey. *Mediterranean Archaeology & Archaeometry* 12(2): 117–131.
- Polymeris GS, Kitis G, Kiyak NG, Theodosoglou E, Tsirliganis NC, Ertek A and Erginal AE, 2016. Dating fossil root cast (Black Sea coast, Turkey) using thermoluminescence: Implications for wind-

- blown drift of shelf carbonates during MIS 2. *Quaternary International* 401: 184–193, DOI [10.1016/j.quaint.2015.05.060](https://doi.org/10.1016/j.quaint.2015.05.060).
- Sadek AM, Eissa HM, Basha AM and Kitis G, 2014. Development of the peak fitting and peak shape methods to analyze the thermoluminescence glow-curves generated with exponential heating function. *Nuclear Instruments & Methods in Physics Research Section B-Beam Interactions With Materials And Atoms* 330: 103–107, DOI [10.1016/j.nimb.2014.04.006](https://doi.org/10.1016/j.nimb.2014.04.006).
- Şahiner E, 2017. Deconvolution analysis of thermoluminescent glow curves in various commercial dosimeters using two different approaches in the framework of the one-trap, one-recombination model. *Turkish Journal of Physics* 41: 477–490, DOI [10.3906/fiz-1704-25](https://doi.org/10.3906/fiz-1704-25).
- Stirling RJ, Duller GAT and Roberts HM, 2014. Developing a single-aliquot protocol for measuring equivalent dose in biogenic carbonates. *Radiation Measurements* 47: 725–731, DOI [10.1016/j.radmeas.2012.01.010](https://doi.org/10.1016/j.radmeas.2012.01.010).
- Wagner GA, 1998. *Age determination of young rocks and artifacts: physical and chemical clocks in quaternary geology and archaeology*. Springer-Verlag, Berlin-Heidelberg.
- Wintle AG, 1977. Thermoluminescence dating of minerals – traps for the unwary. *Journal of Electrostatics* 3: 281–288, DOI [10.1016/0304-3886\(77\)90100-0](https://doi.org/10.1016/0304-3886(77)90100-0).
- Wintle AG, 1978. A thermoluminescence dating study of some Quaternary calcite: potential and problems. *Canadian Journal of Earth Sciences* 15: 1977–1986, DOI [10.1139/e78-208](https://doi.org/10.1139/e78-208).